J. Fluid Mech. (1974), *vol.* 62, *part* 3, *pp.* 553–578
Printed in Great Britain

Computer extension and analytic continuation of Stokes' expansion for gravity waves

By LEONARD W. SCHWARTZ

Department of Aeronautics and Astronautics, Stanford University, California†

(Received 25 April 1973)

Stokes' infinitesimal-wave expansion for steady progressive free-surface waves has been extended to high order using a computer to perform the coefficient arithmetic. Stokes' expansion has been found to be incapable of yielding the highest wave for any value of the water depth since convergence is limited by a square-root branch-point some distance short of the maximum. By reformulating the problem using a different independent parameter, the highest waves are obtained correctly. Series summation and analytic continuation are facilitated by the use of Padé approximants. The method is valid in principle for any finite value of the wavelength and solutions of high accuracy can be obtained for most values of the wave height and water depth. An alternative expansion procedure proposed by Havelock for the computation of waves short of the highest has been reconsidered and found to be defective.

1. Introduction

The problem of steady progressive free-surface waves is one of the oldest in the literature of mathematical fluid mechanics. Gerstner (1804) recognized that the free surface is characterized by constant pressure and offered a simple solution having this property. In the Gerstner wave each fluid particle trajectory is a trochoid. Both the surface and continuity conditions are satisfied exactly, but the flow field is not irrotational. Stokes (1849), after a careful consideration of how wave motion may be excited by surface forces, concluded that the flow of greatest physical interest should be free of rotation. Thus the problem consists of finding a two-dimensional velocity field with constant surface pressure whose velocity components may be derived from a potential function which satisfies Laplace's equation. Stokes proposed a solution by means of a perturbation expansion in a parameter assumed to vary monotonically with the wave height/length ratio. The method yields solutions in which the space co-ordinates are taken as the independent variables.

While preparing his collected papers in 1880, Stokes had occasion to reconsider the method and discovered that the complexity of the calculations could be greatly reduced by using the velocity potential and stream function, rather than the space co-ordinates, as the independent quantities. It is this second method of Stokes which will be considered in the present work.

† Present address: N.A.S.A. Ames Research Center, Moffett Field, California.

Stokes (1880) demonstrated that his perturbation expansion can be computed for finite as well as infinite water depths. He conceded, however, that the series will converge more slowly for smaller values of depth/wavelength. An approximate solution for the extreme case, depth/length approaching zero, called the solitary wave, was found by Boussinesq in 1871. Another approximate solution, for depth/length small, but finite, was given by Korteweg & de Vries (1895). This approximation is known as the cnoidal wave because of its description in terms of the Jacobian elliptic function $\mathrm{cn}(x, k)$. Both the solitary and cnoidal waves were found by Keller (1948) to be derivable from a higher-order extension of the shallow-water theory. From the point of view of flow field computation the high-order shallow-water theory, because of its complexity, is significantly less attractive than the infinitesimal-wave expansion of Stokes.

A number of interesting questions concerning the mathematical character of the steady progressive-wave solution remain to be explored. By a simple argument, Stokes showed that the highest free-surface wave, assumed to be sharp-crested, would have an included angle of 120° at the crest. May one conclude, therefore, that this highest wave represents the limiting value for the small parameter in the infinitesimal-wave expansion? Second, one may ask, to what extent is the Stokes expansion capable of yielding accurate results for high waves in shallow water? Do deep-water and shallow-water waves differ fundamentally in character or merely in scale? These are the questions which have motivated the present study.

Several authors have devised proofs of the existence of periodic gravity waves. Nekrasov (1921) was able to demonstrate that a non-trivial solution to the progressive-wave problem, formulated as an integral equation, could be found for sufficiently small values of the wave amplitude. Levi-Civita, Struik and others did similar work, extending the proof to cover the finite depth case. Krasovskii (1960) has devised by far the most significant proof using techniques from the theory of positive operators. He shows that Nekrasov's equation has solutions, for any value of the depth, for which the maximum surface angle takes on values in the closed interval $[0, \frac{1}{6}\pi]$. He shows further that the Froude number, or dimensionless wave speed, is bounded and assumes its maximum and minimum when the surface angle lies in this interval. However, the proof does not suggest a method of solution and does not rule out the possibility that solutions with surface angles greater than 30° can be found, for example.

Before proceeding, however, it may be well to consider the usefulness of this steady, inviscid, potential flow solution in problems of physical interest. Recent papers by Whitham (1967) and Benjamin & Feir (1967) have considered the stability of an infinite train of progressive Stokes waves with respect to small frequency modulations. They conclude that for sufficiently large values of the water depth slight disturbances to the wave train will grow exponentially. Since these disturbances are always present, the wave train will inevitably disintegrate after a sufficient period of time. This should not be interpreted as implying that Stokes waves in deep water do not exist in nature, but merely that they cannot be expected to preserve a constant form over long time scales.

The process of wave breaking is one of considerable physical importance. In the Stokes theory the wave form is assumed to remain symmetrical as the amplitude increases until the wave of maximum height, for a given wavelength and water depth, is reached. If additional energy is transferred to this sharp-crested wave, the profile will disintegrate, breaking first at the crest. In the open ocean a number of other factors contribute to the breaking phenomenon. The complex process of wind–wave interaction can lead to breaking by energy transfer through the turbulent boundary layer. Moreover, ocean waves propagate on the air–water interface; thus they are subject to shear instabilities of the Kelvin–Helmholtz type. In addition the ocean surface is formed by the superposition of many wave trains of different direction and frequency. The interactions between short gravity waves and large-scale 'carrier' waves can lead to yet other possible breaking mechanisms.

The breaking of waves on beaches is caused primarily by the decreasing depth, which forces the waves to steepen and ultimately break. If the beach slope is small, wave reflexion is minimal and spilling breakers are observed. Since the bottom, in this case, is almost horizontal, we feel that the highest-wave results of the present study should be useful in predicting where the breakers will first be formed.

The present work is envisaged as having a dual objective. While dealing specifically with the problem of Stokes waves, it also serves to illustrate the type of information which may be extracted from a high-order perturbation computation. Often the domain of validity of a power series can be extended far beyond its circle of convergence through the use of Padé approximants (rational fractions). Though Padé approximants have long been recognized as providing a type of 'automatic' analytic continuation, it is only recently, with the advent of modern computers to handle the algebraic drudgery, that their worth as a research tool has been revealed. Another technique of great value in the interpretation of perturbation computations is the graphical procedure of Domb & Sykes (1957). Their method is an extension of the d'Alembert ratio test which, for a class of simple functions, can accurately predict the nature and location of the singularity which limits convergence.

2. The perturbation solution

Consider symmetrical two-dimensional periodic waves moving from right to left with constant speed c relative to an inertial frame on the surface of fluid of finite depth. The bottom is assumed to be horizontal. Consider a second frame of reference moving with a wave crest. With respect to this frame the motion is steady; the general direction of flow is now from left to right. The fluid is assumed to be inviscid and incompressible and the motion to be irrotational; hence the solution may be represented as an analytic function of the complex variable z. One cycle in the physical or z plane is shown in figure 1 (a). In the figure L is the wavelength, D the mean depth measured from the still-water level and A the peak-to-trough wave height. g, the acceleration due to gravity, acts downward. The y axis is known to be a line of symmetry. The wave speed c may be defined as

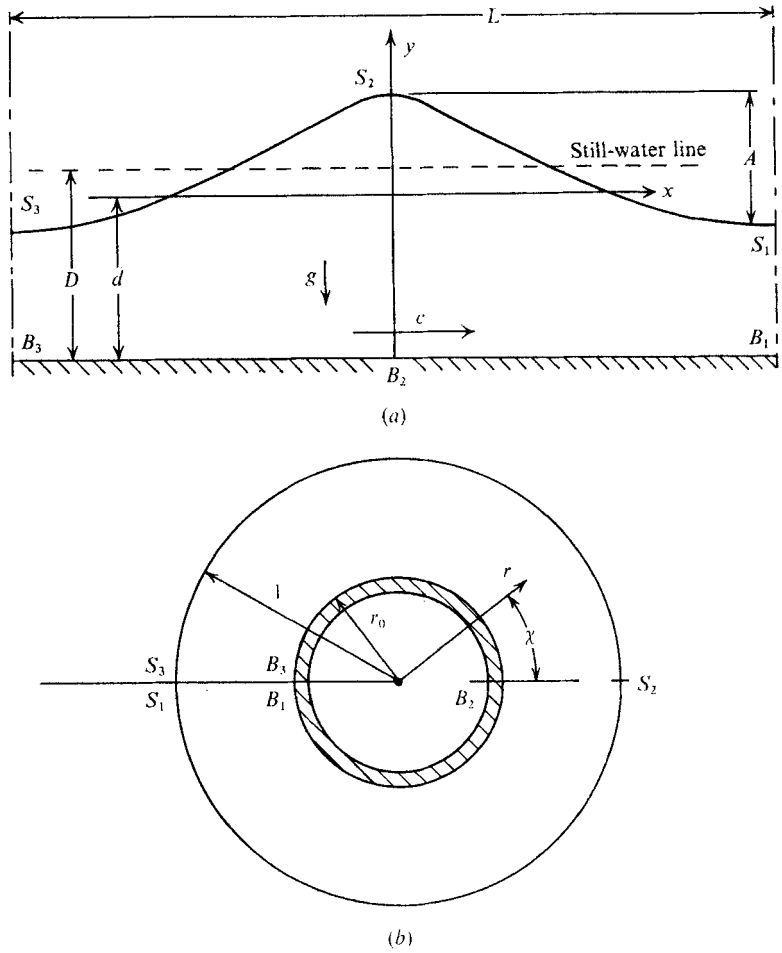

FIGURE 1. (*a*) z plane, (*b*) ζ plane.

the average fluid velocity at any horizontal level completely within the fluid. That is,

$$c = \frac{1}{L}\int_{x}^{x+L} u(x, y)\, dx \tag{2.1}$$

in the wave-fixed reference frame.

Introduce dimensionless variables by selecting $c_0 = (gL/2\pi)^{\frac{1}{2}}$ as the reference velocity and $L/2\pi$ as the reference length. Let the stream function ψ assume the values 0 and $-Q$ on the free surface and channel bottom respectively. Locate the x axis a distance $d = Q/c$ above the bottom. This undisturbed fluid depth d will in general differ from the mean depth D by the small amount $\bar{y}$. The quantity $\bar{y}L$ is the fluid volume convected by each wave cycle by virtue of the definition of the wave speed c. The Bernoulli condition is imposed on the unknown free surface;

$$q\bar{q} + 2y = K \quad \text{on} \quad \psi = 0, \tag{2.2}$$

where $q = u - iv$ and the bar signifies complex conjugation.

Rather than solve the problem in the physical plane, where the shape of the

free surface is unknown, we map the interior of each fluid cycle in the z plane into an annulus of unit outer radius in the ζ plane according to the transformation

$$z(\zeta) = i[\log\zeta + a_1(\zeta - r_0^2/\zeta) + \ldots + (a_j/j)(\zeta^j - r_0^{2j}/\zeta^j) + \ldots], \tag{2.3}$$

where $\zeta = re^{i\chi}$. The channel bottom $\psi = -cd$ and free surface $\psi = 0$ are mapped onto the circles $r = e^{-d}$ and $r = 1$ respectively. The ζ-plane solution is a simple potential vortex

$$w = \phi + i\psi = ic\log\zeta. \tag{2.4}$$

Equations (2.3) and (2.4) effect the exchange of roles of the independent and dependent variables analogous to the procedure of Stokes (1880). The resulting problem in the ζ plane is quadratically rather than exponentially nonlinear and the perturbation calculations are considerably simplified. Figure 1 (*b*) shows the ζ plane. Corresponding points in figures 1 (*a*) and (*b*) are denoted by the same symbols. Note that the branch cut in figure 1 (*b*) separates different wave cycles corresponding to multiple values of $\log\zeta$ in (2.3).

The free-surface wave problem as formulated will have a two-parameter family of solutions depending, in general, on the transformed water depth r_0 and the wave height A. The limiting cases $r_0 = 0$ and $r_0 = 1$ represent deep-water and solitary waves respectively.

The unknown transformation coefficients a_j in (2.3) are determined by condition (2.2) rewritten in the new variables. The velocity may be calculated as

$$q = \frac{dw}{dz} = \frac{dw/d\zeta}{dz/d\zeta} = \frac{c}{1 + a_1(\zeta + r_0^2/\zeta) + \ldots + a_j(\zeta^j + r_0^2/\zeta^j) + \ldots}. \tag{2.5}$$

Expressions for the free-surface velocity and elevation are obtained by setting $\zeta = e^{i\chi}$ in (2.5) and the imaginary part of (2.3). Equation (2.2) can then be written as a cosine series in χ. Setting the separate harmonic coefficients equal to zero, we obtain

$$c^2 + 2\sum_{l=1}^{\infty} \frac{a_l\delta_l f_l}{l} = Kf_0, \tag{2.6a}$$

$$\sum_{i=1}^{\infty} \frac{a_l\delta_l}{l}\{f_{|l-j|} + f_{j+l}\} = Kf_j \quad (j = 1, 2, \ldots). \tag{2.6b}$$

The f_i have been introduced for convenience and need not be reported in the final solution. They are defined as

$$f_0 = 1 + \sum_{l=1}^{\infty} a_l^2\sigma_{2l}, \tag{2.7a}$$

$$f_1 = a_1\sigma_1 + \sum_{l=1}^{\infty} a_l a_{l+1}\sigma_{2l+1}, \tag{2.7b}$$

$$f_i = a_i\sigma_i + \sum_{l=1}^{\infty} a_l a_{l+i}\sigma_{2l+i} + \frac{1}{2}\sum_{l=1}^{i-1} a_l a_{i-l}(\sigma_l - \delta_{i-l}) \quad (i = 2, 3, \ldots), \tag{2.7c}$$

where $\sigma_i = 1 + r_0^{2i}$ and $\delta_i = 1 - r_0^{2i}$ for $i \geqslant 1$. Equations (2.6) and (2.7) completely determine the a_i, c^2 and K for a given wave height and water depth. They will be

solved by a high-order perturbation calculation where the digital computer is used to find and store the coefficients.

Let ϵ be a global parameter associated with the wave height that is equal to zero when A equals zero. A more explicit definition of ϵ will be deferred for the moment. Assume power-series expansions in ϵ of the form

$$a_j = \sum_{k=0}^{\infty} \alpha_{jk} \epsilon^{j+2k} \quad (j = 1, 2, \ldots), \tag{2.8a}$$

$$f_j = \sum_{k=0}^{\infty} \beta_{jk} \epsilon^{j+2k} \quad (j = 0, 1, \ldots), \tag{2.8b}$$

$$c^2 = \sum_{l=0}^{\infty} \gamma_l \epsilon^{2l}, \quad K = \sum_{l=0}^{\infty} \Delta_l \epsilon^{2l}. \tag{2.8c,d}$$

Expansions (2.8) are substituted in (2.6) and (2.7) and, by equating coefficients of like powers of ϵ, recurrence relations for the α's, β's, γ's and Δ's are obtained. These are

$$\gamma_l + 2 \sum_{r=0}^{l-1} \frac{\delta_{l-r}}{l-r} \sum_{m=0}^{r} \alpha_{l-r,r-m} \beta_{l-r,m} = \sum_{k=0}^{l} \Delta_{l-k} \beta_{0k} \quad (l = 0, 1, \ldots), \tag{2.9a}$$

$$\sum_{l=1}^{j} \frac{\delta_l}{l} \sum_{s=0}^{p} \alpha_{l,p-s} \beta_{j-l,s} + \sum_{l=1}^{p} \frac{\delta_{l+j}}{l+j} \sum_{s=0}^{p-l} \alpha_{l+j,p-l-s} \beta_{ls} + \sum_{l=0}^{p-1} \frac{\delta_{p-l}}{p-l} \sum_{s=0}^{l} \alpha_{p-l,l-s} \beta_{j+p-l,s}$$

$$= \sum_{l=0}^{p} \Delta_l \beta_{j,p-l} \quad (p = 0, 1, \ldots, \quad j = 1, 2, \ldots), \tag{2.9b}$$

$$\beta_{00} = 1, \quad \beta_{0k} = \sum_{l=1}^{k} \sigma_{2l} \sum_{r=0}^{k-l} \alpha_{lr} \alpha_{l,k-l-r} \quad (k = 1, 2, \ldots), \tag{2.9c}$$

$$\beta_{jk} = \alpha_{jk} \sigma_j + \sum_{l=1}^{k} \sigma_{2l+j} \sum_{r=0}^{k-l} \alpha_{lr} \alpha_{l+j,k-l-r}$$

$$+ \frac{1}{2} \sum_{l=1}^{j-1} (\sigma_l - \delta_{j-l}) \sum_{r=0}^{k} \alpha_{lr} \alpha_{j-l,k-r} \quad (j = 1, 2, \ldots, \quad k = 0, 1, \ldots), \tag{2.9d}$$

where summations are taken to be identically zero in those cases where the lower limit exceeds the upper. Equations (2.9c) and (2.9d), defining the relationship between the α's and the β's, are derived from (2.7). Equations (2.9a) and (2.9b) come from (2.6). The system of equations (2.9) is not closed until the parameter ϵ is identified.

3. Extension of Stokes' solution

If we choose $\epsilon = a_1$, the first transformation coefficient in (2.3), we in effect reproduce the expansion procedure of Stokes (1880). The system of equations (2.9) is closed by taking

$$\alpha_{10} = 1, \quad \alpha_{1k} = 0 \quad (k = 1, 2, \ldots).$$

Stokes himself computed the solution to $O(a_1^3)$ for general depth and to $O(a_1^5)$ in the special case of infinite depth. Wilton (1914) carried the infinite depth computation up to $O(a_1^{10})$ but has errors starting with his eighth-order results. De (1955)

has published a fifth-order solution for general depth. These last two suggest the order of solution which is the practical limit of hand calculation.

Equations (2.9) were programmed in FORTRAN IV and solved to high order on the Stanford 360/67 computer. The execution time for a double-precision (16 decimal place) solution to order a_1^{70} was just under one minute. The value of the water depth, corresponding to the input parameter r_0, does not affect the run time.

The most significant derived parameter in this formulation is the peak-to-trough wave height. The wave profile in the z plane may be obtained parametrically in terms of the angle χ by substituting $\zeta = e^{i\chi}$ into (2.3) and separately equating real and imaginary parts. We obtain

$$y = a_1\delta_1\cos\chi + \tfrac{1}{2}a_2\delta_2\cos 2\chi + \ldots + (a_n\delta_n/n)\cos n\chi + \ldots, \tag{3.1a}$$

$$-x = \chi + a_1\sigma_1\sin\chi + \tfrac{1}{2}a_2\sigma_2\sin 2\chi + \ldots + (a_n\sigma_n/n)\sin n\chi + \ldots. \tag{3.1b}$$

Since peaks correspond to $\chi = 0$ and troughs to $\chi = \pi$, the semi-wave height is given by

$$h = \tfrac{1}{2}[y(0) - y(\pi)] = a_1\delta_1 + \tfrac{1}{3}a_3\delta_3 + \ldots = \sum_{j=1}^{\infty}(a_{2j-1}\delta_{2j-1})/(2j-1). \tag{3.2}$$

Or, by expanding the a_i in powers of ϵ and regrouping, we obtain

$$h = \sum_{q=1}^{\infty}\eta_q\epsilon^{2q-1} \quad \text{where} \quad \eta_q = \sum_{j=1}^{q}(\alpha_{2j-1,\,q-j}\delta_{2j-1})/(2j-1). \tag{3.3}$$

Note that h is equal to $\pi A/L$. The results up to $O(a_1^8)$ for the deep-water wave, $r_0 = 0$, are presented below. Rational numbers were obtained by recognizing repeating patterns in the computer-produced decimals.

$$\left.\begin{aligned}
a_1 &= a_1,\\
a_2 &= 2a_1^2 + a_1^4 + \tfrac{29}{6}a_1^6 + \tfrac{1123}{36}a_1^8 + \ldots,\\
a_3 &= \tfrac{9}{2}a_1^3 + \tfrac{19}{4}a_1^5 + \tfrac{1183}{48}a_1^7 + \ldots,\\
a_4 &= \tfrac{32}{3}a_1^4 + \tfrac{313}{18}a_1^6 + \tfrac{103727}{1080}a_1^8 + \ldots,\\
a_5 &= \tfrac{625}{24}a_1^5 + \tfrac{16603}{288}a_1^7 + \ldots,\\
a_6 &= \tfrac{342}{5}a_1^6 + \tfrac{54473}{300}a_1^8 + \ldots,\\
a_7 &= \tfrac{117649}{720}a_1^7 + \ldots, \quad a_8 = \tfrac{131072}{315}a_1^8 + \ldots,\\
K &= 1 + 2a_1^2 + \tfrac{11}{2}a_1^4 + \tfrac{167}{6}a_1^6 + \tfrac{26137}{144}a_1^8 + \ldots,\\
c^2 &= 1 + a_1^2 + \tfrac{7}{2}a_1^4 + \tfrac{229}{12}a_1^6 + \tfrac{6175}{48}a_1^8 + \ldots,\\
h &= a_1 + \tfrac{3}{2}a_1^3 + \tfrac{163}{24}a_1^5 + \tfrac{62047}{1440}a_1^7 + \ldots.
\end{aligned}\right\} \tag{3.4}$$

Wilton noticed that the first coefficient in the expansion for each a_n is given by $n^n/n!$. Note that the last coefficient shown, for both K and c^2, does not agree with his results.

The displacement of the still-water level and hence the mass transport may be computed once the a_j are known. By definition

$$\bar{y} \equiv D - d = \frac{1}{\pi}\left[\int_0^{\pi} y\,dx\right]_{\psi=0}. \tag{3.5}$$

Using the parametric representations of x and y given in (3.1) and performing the integration yields

$$\bar{y} = (\tfrac{1}{2}) \sum_{j=1}^{\infty} \frac{\delta_{2j} a_j^2}{j}. \tag{3.6}$$

This last equation can then be rewritten as a series in ϵ.

Inspection of each series in (3.4) reveals a trend which continues into the higher-order solution. All the coefficients are positive, implying that the singularity which limits convergence corresponds to a positive real value of a_1^2 and that each dependent quantity in (3.4) is monotonically increasing up to this critical value. Stokes conjectured that this singularity would correspond to the highest possible wave, which has the 120° crest angle.

In order to determine the nature and location of this limiting singularity we employ a graphical procedure due to Domb & Sykes (1957). They note that if

$$f(\epsilon) = \sum_{n=0}^{\infty} a_n \epsilon^n = \begin{cases} K(\epsilon_0 \pm \epsilon)^\alpha, & \alpha \neq 0, 1, \ldots, \\ K(\epsilon_0 \pm \epsilon)^\alpha \log(\epsilon_0 \pm \epsilon), & \alpha = 0, 1, \ldots, \end{cases} \tag{3.7a}$$

then

$$a_n/a_{n-1} = \mp \epsilon_0^{-1}[1 - (1+\alpha)/n], \tag{3.7b}$$

which follows from the binomial expansion. Thus, for these special cases, if we plot the ratios a_n/a_{n-1} versus $1/n$, the points will lie on a straight line. In general the unknown function f can be thought of as the sum of a number of singularities. If the one closest to the origin of ϵ is of the above type, then the Domb–Sykes plot will ultimately tend towards a straight line as $1/n$ becomes small. The vertical intercept determines the reciprocal of the radius of convergence while the horizontal intercept $1/n = 1/(1+\alpha)$ yields the singularity exponent.

In figure 2 we show Domb–Sykes plots for the semi-wave height series (3.3) for three depths. In each case the ratios of series coefficients asymptote to straight lines. All three asymptotes have the same horizontal intercept $1/n = \frac{2}{3}$. Thus in each case the series convergence is limited by a square-root branch-point at a critical value $a_1^*(r_0)$. Thus the form of $h(a_1)$ in the vicinity of the branch-point is

$$h(a_1; r_0) \sim a_1[a_1^{*2}(r_0) - a_1^2]^{\frac{1}{2}}. \tag{3.8}$$

The same critical values $a_1^*(r_0)$ are obtained for other dependent quantities. For the case of infinite depth, the plot gives the critical value $a_1^* = 0{\cdot}2972$.

Several investigators have computed the highest-wave profile for the case of infinite depth. They exploit the fact that the 120° crest angle is known and build it into their solutions. In the ζ plane the wave peak is found at the point $\zeta = 1$. For the highest wave, from the surface condition and dimensional homogeneity, one can find the local solution

$$q = dw/dz \sim (1-\zeta)^{\frac{1}{3}} \tag{3.9}$$

near the wave crest. If the computation is restricted to the highest wave in deep water, the factor $(1-\zeta)^{\frac{1}{3}}$ may be inserted on the right side of (2.5), thereby ensuring that the wave profile has the proper crest. The methods of Michell (1893), later extended by Havelock (1919), and Yamada (1957*a*) proceed in this fashion. In each case the Bernoulli condition is then manipulated to yield relations which may be used to determine the unknown series coefficients. The Michell–

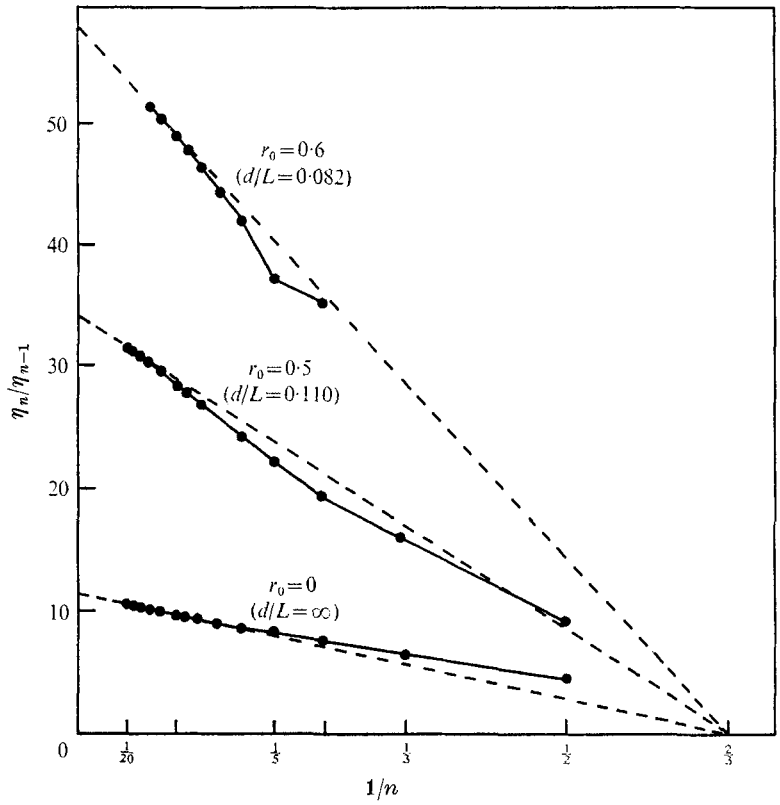

FIGURE 2. Domb–Sykes plot for wave height $h = \sum_{n=1} \eta_n a_1^{2n-1}$.

Havelock method uses the first coefficient $\beta_1 = \frac{1}{3} - a_1$ as an expansion 'parameter' and expresses succeeding coefficients as power series in this quantity. At each stage of solution β_1 is re-evaluated. Havelock's fourth-order computation gives $a_1 = 0{\cdot}2919$ and a maximum wave height $(A/L)_{\max} = 0{\cdot}1418$. Havelock offers the first number as the critical value for the Stokes expansion. We have repeated his work up to fourth order and find $a_1 = 0{\cdot}2920$ and $(A/L)_{\max} = 0{\cdot}1417$ at that stage. The successive estimates for these numbers form a decreasing sequence, suggesting that the final values will be slightly below those given. Yamada's approach is somewhat different. He truncates the unknown series, retaining only the first twelve elements. By an iterative computation he obtains optimum values satisfying the surface condition at a number of points on the wave profile. His results give $a_1 = 0{\cdot}2921$ and $(A/L)_{\max} = 0{\cdot}1412$.

The utility of our high-order series solution is greatly increased by recasting the polynomials as Padé approximants (rational fractions). From a typical series of the form

$$f(\epsilon) = a_0 + a_1\epsilon + \ldots + a_{M+N}\epsilon^{M+N} + \ldots, \tag{3.10}$$

we can form the rational fraction

$$[N, M]f(\epsilon) = \frac{b_0 + b_1\epsilon + \ldots + b_M\epsilon^M}{1 + c_1\epsilon + \ldots + c_N\epsilon^N}, \tag{3.11}$$

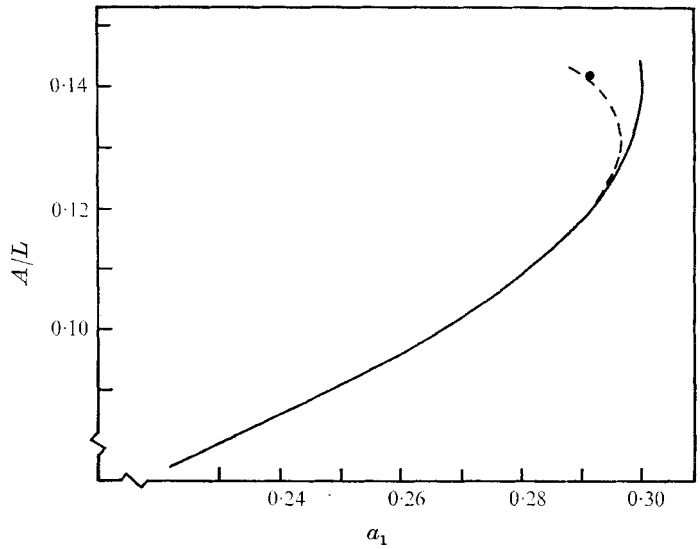

FIGURE 3. Direct and reverted series for the wave height h and the first transformation coefficient a_1; infinite depth. ——, direct, $h = [9,9]h(a_1)$; – – –, reverted, $a_1 = [9,9]a_1(h)$; ●, highest wave of Havelock (1919).

where the coefficients b_j and c_j are uniquely determined by the a_j for given M and N. The most important special case is when the orders of the numerator and denominator are equal. The series (3.10) will converge to a limit only if ϵ lies within a circle whose radius is determined by the location of the nearest singularity in the complex-ϵ plane. The sequence of Padé approximants $[N,N]f(\epsilon), N = 1,2,\ldots,$ will, in general, converge in a much larger domain, the shape of which is determined by the branch-points of f. The $[N,N]$ fractions provide rational approximations to the analytic continuation of the power series. This is due primarily to their invariance under the Euler transformation

$$\bar{\epsilon} = \epsilon/(\epsilon_0 - \epsilon), \tag{3.12}$$

where ϵ_0 is not zero but is otherwise arbitrary. Though the theory of Padé fractions is not completely understood, their use is indicated when a significant number of series coefficients have been computed. Baker (1965) gives examples of their successful application in a variety of physical problems.

Figure 3 is a plot of wave height versus a_1 computed as a [9, 9] approximant formed from the series solution. Havelock's highest-wave result, where this curve had been assumed to terminate, is shown as a point in the figure. The curve misses Havelock's point by a good deal. The square-root branch-point of (3.8) can be removed by reverting $h(a_1)$ to obtain a single-valued function $a_1(h)$. The reverted series has also been recast as a [9, 9] approximant. Its graph is seen to pass quite close to Havelock's point. Thus while Havelock's procedure in all probability finds the highest wave correctly, the value of a_1 he determined is not the critical one for the Stokes expansion. Analogous results have been found for the finite depth cases.

4. Perturbation series in the wave height

This defect in the Stokes expansion can be removed by substituting the reverted series $a_1(h)$ into the other series in (3.4). However, because of the round-off error inherent in this process, it is preferable to reformulate the problem using the wave height itself as the independent parameter. Thus we take $\epsilon = h$ and add (3.3) with $\eta_1 = 1$ and $\eta_k = 0$, $k = 2, 3, \ldots$, to the system (2.9) to produce closure. Apart from this small modification the computation procedure previously outlined still applies and the run time is identical. Solutions to $O(h^{48})$ were computed for values of the depth parameter r_0 ranging from 0·1 to 0·9 by intervals of 0·1. For the special case of infinite depth the solution was found to $O(h^{117})$.

As before, for the deep-water wave, we can recognize the first few coefficients as rational numbers from their repeating decimals. To ninth order the results are

$$\left.\begin{aligned}
a_1 &= h - \tfrac{3}{2}h^3 - \tfrac{1}{24}h^5 - \tfrac{3007}{1440}h^7 - \tfrac{1617319}{302400}h^9 - \ldots,\\
a_2 &= 2h^2 - 5h^4 + \tfrac{19}{6}h^6 - \tfrac{283}{40}h^8 - \tfrac{165617}{16800}h^{10} - \ldots,\\
a_3 &= \tfrac{9}{2}h^3 - \tfrac{31}{2}h^5 + \tfrac{113}{6}h^7 - \tfrac{42521}{1440}h^9 - \ldots,\\
a_4 &= \tfrac{32}{3}h^4 - \tfrac{839}{18}h^6 + \tfrac{88307}{1080}h^8 - \ldots, \quad a_5 = \tfrac{625}{24}h^5 - \tfrac{39647}{288}h^7 + \tfrac{5396111}{17280}h^9 - \ldots,\\
a_6 &= \tfrac{324}{5}h^6 - \tfrac{120487}{300}h^8 + \ldots, \quad a_7 = \tfrac{117649}{720}h^7 - \tfrac{50164867}{43200}h^9 + \ldots,\\
a_8 &= \tfrac{131072}{315}h^8 - \ldots, \quad a_9 = \tfrac{14348907}{13440}h^9 - \ldots,\\
c^2 &= 1 + h^2 + \tfrac{1}{2}h^4 + \tfrac{1}{4}h^6 - \tfrac{22}{45}h^8 - \tfrac{1150069}{25200}h^{10} - \ldots,\\
K &= 1 + 2h^2 - \tfrac{1}{2}h^4 - \tfrac{5}{6}h^6 - \tfrac{301}{80}h^8 - \tfrac{7739111}{50400}h^{10} - \ldots,\\
S &= 1 + h + 2h^2 + 3h^3 + \tfrac{17}{3}h^4 + \tfrac{21}{2}h^5 + \tfrac{961}{45}h^6 + \tfrac{2549}{60}h^7 + \tfrac{842647}{9450}h^8 + \tfrac{128661}{700}h^9 + \ldots.
\end{aligned}\right\} \tag{4.1}$$

Results up to order thirty for both the deep-water wave and the case $r_0 = 0{\cdot}5$ corresponding to the depth/wavelength ratio $d/L = 0{\cdot}110$ may be found in the author's Ph.D. dissertation (1972).

The maximum wave height ratio $(A/L)_{\max}$ can be obtained, for each depth, by exploiting the fact that the sharp crest of the highest wave is a stagnation point. The crest velocity is given by (2.5) with $\zeta = 1$. Thus

$$q_{\text{crest}} = c/S, \tag{4.2}$$

where

$$S = 1 + \sum_{j=1}^{\infty} a_j \sigma_j = \sum_{j=0}^{\infty} s_j h^j \tag{4.3a}$$

and

$$s_0 = 1, \quad s_j = \sum_{k=0}^{[\frac{1}{2}(j-1)]} \alpha_{j-2k,\,k}\,\sigma_{j-2k}. \tag{4.3b}$$

Here $[A]$ signifies the greatest integer not exceeding A. Since q_{crest} is zero for the highest wave and c is known to be bounded (Krasovskii 1960), the series expansion for S must become singular at the critical value of h.

Figure 4 shows Domb–Sykes plots of the ratios s_j/s_{j-1} for three depths. The vertical intercept of the extrapolated curve gives an estimate of $h_{\max}$ for each case. Notice that the curves for $r_0 = 0$ and 0·2 show damped oscillations of period two while for $r_0 = 0{\cdot}3$ the period is four. For $r_0 = 0$ the intercept is about 2·25, corresponding to $(A/L)_{\max} = 0{\cdot}141$.

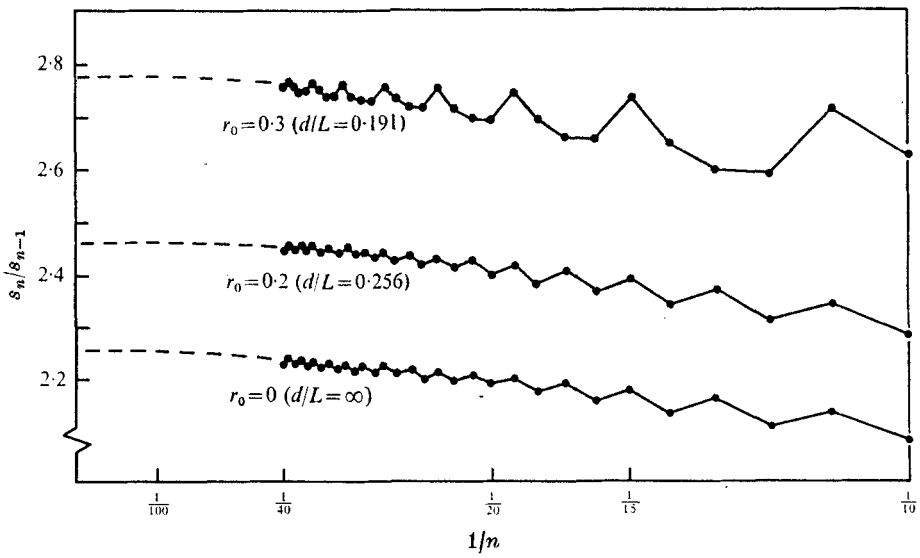

FIGURE 4. Domb–Sykes plot of the expansion for $S = c/q_{\text{crest}} = \sum_{n=0}^{\infty} s_n h^n$ for three depths.

The oscillations in these curves are caused by the presence of other singularities in the h plane. A singularity on the negative real axis somewhat further away from the origin than the one at $h_{\max}$ is responsible for the damped oscillation of period two in the curves for $r_0 = 0$ and 0·2. For $r_0 = 0{\cdot}3$, these two singularities are augmented by a conjugate pair on the imaginary axis. If we had plotted, instead, the ratios s_{2j}/s_{2j-2} we should have obtained smooth curves for $r_0 = 0$ and 0·2 and a curve with period two for $r_0 = 0{\cdot}3$. Each original series would become two series, one for the odd- and one for the even-order terms:

$$S(h) = h \sum_{j=0}^{\infty} s_{2j+1} h^{2j} + \sum_{j=0}^{\infty} s_{2j} h^{2j}. \tag{4.4}$$

By using the variable h^2, rather than h, the singularities on the negative real axis are mapped onto the positive axis behind the leading one at $h^2_{\max}$; hence the period-two oscillation disappears.

The maximum wave height for the deep-water wave may be estimated from the coefficients in either series on the right-hand side of (4.4). The sequences $\{A_j\} = \{s_{2j+1}/s_{2j-1}\}$ and $\{B_j\} = \{s_{2j}/s_{2j-2}\}$, $j = 1, 2, \ldots$, each converge monotonically to the reciprocal of $h^2_{\max}$. Their convergence may be accelerated by application of the nonlinear transformation of Shanks (1955). The coefficient ratios were computed for $j \leqslant 35$ and 36 for the odd- and even-order sequences respectively. From the last five elements in each sequence table 1 may be constructed; the operator e_1 is defined by

$$e_1(A_n) = \frac{A_{n+1}A_{n-1} - A_n^2}{A_{n+1} + A_{n-1} - 2A_n}. \tag{4.5}$$

A_j	$e_1(A_j)$	$e_1^2(A_j)$	B_j	$e_1(B_j)$	$e_1^2(B_j)$
5·0546	—	—	5·0532	—	—
5·0570	5·0817	—	5·0556	5·0819	—
5·0591	5·0823	5·0822	5·0578	5·0817	5·0819
5·0610	5·0821	—	5·0599	5·0824	—
5·0628	—	—	5·0617	—	—

TABLE 1

The Shanks transformation is equivalent to the assumption that the members of each set of three consecutive elements in the sequences lie in a geometric progression. The entries in each half of the table converge to the number 5·082, corresponding to

$$(A/L)_{\max} = 0{\cdot}1412.$$

This last figure agrees to four decimal places with Yamada's result.

The same procedure can be used for the finite depth cases subject to certain qualifications. The conjugate pair of imaginary singularities in the h plane which is responsible for the additional oscillation in the curve for $r_0 = 0{\cdot}3$ in figure 4 moves ever closer to the origin as the depth is reduced. For $r_0 > 0{\cdot}32$ it is closer even than the highest-wave singularity and so it defines the radius of convergence of the expansion in h. It is spurious, however, and cannot be found in the extension of the Stokes solution, where a_1 rather than h is used as the independent parameter. Thus for $r_0 > 0{\cdot}32$ the sequences $\{s_{2j+1}/s_{2j-1}\}$ and $\{s_{2j}/s_{2j-2}\}$ would not converge to $1/h_{\max}^2$ but rather would indicate the spurious singularity corresponding to negative values of h^2. This difficulty can be overcome by mapping away the offending point by means of an Euler transformation as in (3.12). The above procedure can then be applied to the transformed series. Another method, using $[N, N]$ Padé approximants, is both simpler and more accurate. It will be described below.

We have not been able to specify the nature of the singularity at $h_{\max}$. Horizontal asymptotes to the Domb–Sykes plots in figure 3 seem plausible, suggesting the existence of a simple pole at the critical point. An isolated singular point must be rejected however. For if $h_{\max}$ were such a point it would then be possible to continue analytically the solution around it to obtain real, single-valued results for S and other physical quantities for real $h > h_{\max}$. We expect all physical quantities to have branch-points at $h_{\max}$. The branch cuts emanating from $h_{\max}$ could then shield the portion of the real axis $h > h_{\max}$ from an expansion about the origin.

Shanks (1955) states that Padé approximants place a branch cut in the 'shadow of a branch-point'. That is, the fractions model the branch cut by alternating poles and zeros along an outward ray emanating from the branch-point and collinear with the point of expansion. On the 'cut' the values of the fraction oscillate between zero and infinity as if to emphasize that the function being modelled is not single-valued there. Two sequences of $[N, N]$ approximants have been formed from the odd- and even-order series for S in (4.4). A polynomial factorization routine is then used to locate the poles and zeros of each

approximant. As expected a 'cut' forms on the positive real axis of h^2. Since S becomes infinite at $h_{\max}$ the first element in the cut is a pole. As N increases this leading pole moves monotonically inward, converging ultimately to $h^2_{\max}$. For the deep-water wave we get the following locations for the pole closest to the origin in the h^2 plane. From the even-order series, as N increases from 2 to 11, we obtain the sequence

$$\{0{\cdot}23057,\ 0{\cdot}20953,\ 0{\cdot}20244,\ 0{\cdot}19939,\ 0{\cdot}19794,\ 0{\cdot}19722,\ 0{\cdot}19688,\ 0{\cdot}19674,\ 0{\cdot}19671,\ 0{\cdot}19671\}$$

and from the odd-order series, for the same values of N,

$$\{0{\cdot}22163,\ 0{\cdot}20691,\ 0{\cdot}20144,\ 0{\cdot}19897,\ 0{\cdot}19775,\ 0{\cdot}19713,\ 0{\cdot}19684,\ 0{\cdot}19673,\ 0{\cdot}19671,\ 0{\cdot}19671\}.$$

Thus each sequence converges to the same value. From this number we obtain

$$(A/L)_{\max} = 0{\cdot}14118 \quad \text{for} \quad d/L = \infty. \tag{4.6}$$

5. Finite depth results

The same method has been applied to the finite depth cases to provide highest-wave estimates. For $r_0 = 0{\cdot}1$, $0{\cdot}2$ and $0{\cdot}3$ the sequence of leading pole locations converges to four places for both odd and even orders. As the depth is decreased another branch cut appears on the negative real axis of the h^2 plane. This cut corresponds to the spurious singularity which defines the radius of convergence of the h expansion for $r_0 > 0{\cdot}32$. Since some of the poles of the $[N, N]$ approximants are used for its description, fewer poles are left to simulate the singularities on the positive axis. The net effect is to slow down the rate at which the leading positive pole converges to $h_{\max}$. Shanks's iterated e_1 transformations were used to accelerate convergence for $r_0 \geqslant 0{\cdot}4$. Internal consistency suggests three-place accuracy for $r_0 = 0{\cdot}4$, $0{\cdot}5$ and $0{\cdot}6$, while only two good places could be obtained for $r_0 = 0{\cdot}7$. No highest-wave estimates were possible for $r_0 = 0{\cdot}8$ or $0{\cdot}9$.

Figure 5 compares results of the present work with those of the Michell–Havelock method, extended to finite depth by Chappelear (1959), and those of Yamada & Shiotani (1968), who used the method of Yamada's earlier work. Our highest-wave estimates are indistinguishable from those of Yamada & Shiotani for $r_0 \leqslant 0{\cdot}6$. For $r_0 = 0{\cdot}7$ our results are about 2 % higher. Chappelear's results are consistantly higher owing perhaps to the fact that he carries the Michell–Havelock method to only the third approximation. The radius of convergence of the series expansion in h is also shown. Though spurious, this singularity dominates the series coefficients for shallow water depths.

In table 2 we present, for each value of r_0, the radii of convergence a_1^* and $(A/L)^*$ of the series expansions in a_1 and h. When these values are less than $(a_1)_{\max}$ or $(A/L)_{\max}$, and these latter values are known, we show them in parentheses immediately below the critical values. We also show the corresponding ratio A/d, the wave amplitude divided by the depth, for each point. Empty brackets in the table mean that the value is unknown. It is possible to extrapolate

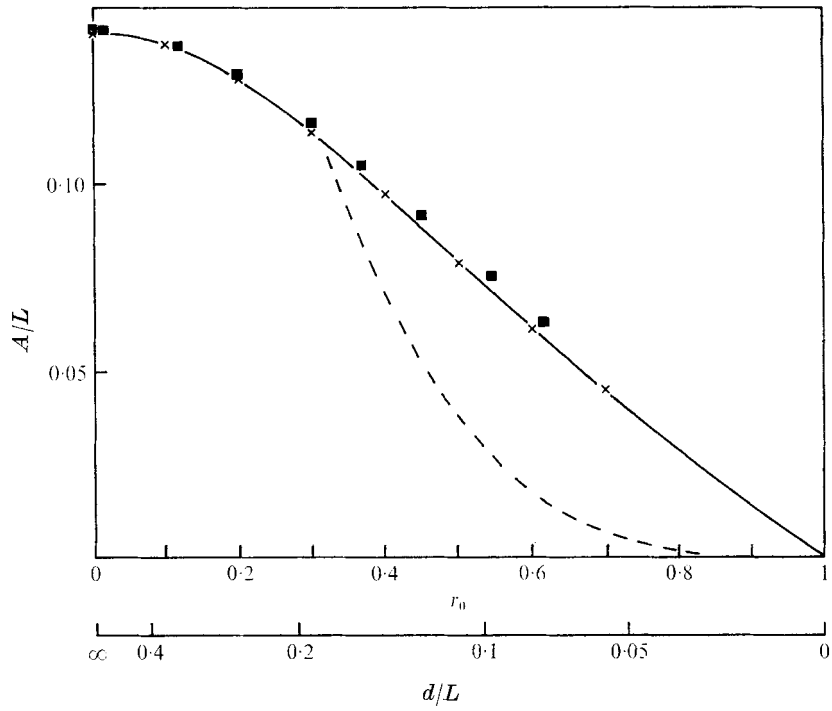

FIGURE 5. Comparison of highest-wave estimates as a function of water depth. $(A/L)_{\max}$: ×, by poles of $[N, N]S(h)$; ■, Chappelear (1959); ——, Yamada & Shiotani (1968). – – –, radius of convergence of expansion in h.

r_0	d/L	a_1^*	A/d	$(A/L)^*$	A/d
0	∞	0·2972	0	0·14118	0
0·1	0·366	0·291	0·347	0·1380	0·377
0·2	0·256	0·274	0·462	0·1285	0·502
0·3	0·191	0·246	0·540	0·1145	0·598
0·4	0·146	0·211	0·595	0·0707	0·484
				(0·0975)	(0·667)
0·5	0·110	0·172	0·624	0·0381	0·345
				(0·0791)	(0·717)
0·6	0·0815	0·131	0·639	0·01803	0·223
				(0·0614)	(0·754)
0·7	0·0570	0·092	0·657	0·00695	0·122
				(0·045)	(0·79)
0·8	0·0356	0·042	0·26	0·00185	0·0520
		(0·056)	( )	( )	( )
0·9	0·0168	0·011	0·08	0·00020	0·0119
		( )	( )	( )	( )

TABLE 2. Radii of convergence of the series expansions

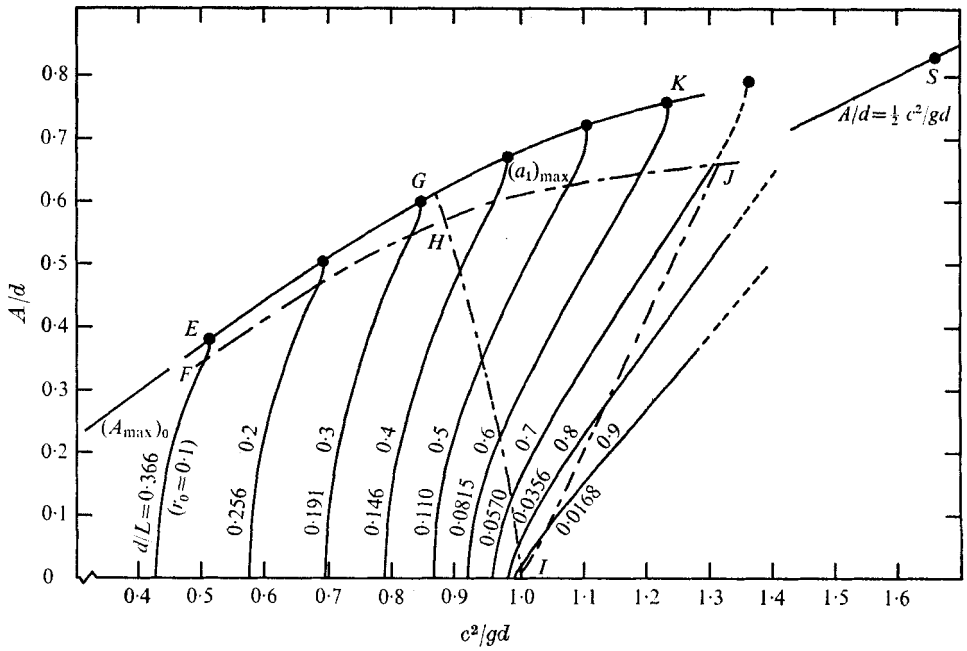

FIGURE 6. Wave velocity *vs.* amplitude and depth (including domains of convergence). ●, highest wave; ——, convergence boundaries; – – –, incomplete convergence.

with reasonable accuracy, but we show only those numbers we have actually computed. All values are correct to the number of places shown.

Notice that the expansions in a_1 do not converge through $(a_1)_{\max}$ for $d/L < 0{\cdot}05$. For very shallow water, the radii of convergence of both expansions decrease with the depth, becoming identically zero for the solitary wave. This is not unexpected, and follows from choosing the wavelength as the reference dimension.

A direct measure of the nonlinearity of the free-surface wave problem is given by the variation in wave speed with amplitude. Figure 6 shows the amplitude ratio A/d versus the square of the dimensionless wave speed, or Froude number referred to the depth c^2/gd, for each value of d/L. This type of plot, which is very efficient for the display of finite depth results, is adapted from Wehausen (1965).

The values of the Froude number, for each r_0, were computed as the Padé fraction $[12, 12]c^2(h)$. In general $[N, N]c^2(h)$ converged well up to amplitudes about 3 % short of the maximum. The speed at $(A/d)_{\max}$ was found, in each case, by extrapolating over this short distance. Thus there is some uncertainty as to the slope of the curves at these points. The highest-wave curve EGK is formed by connecting the limit points. On the dashed extensions of the curves for $r_0 = 0{\cdot}7$, $0{\cdot}8$ and $0{\cdot}9$ the sequences of approximants converged less well, but we feel that the Froude number is still accurate to 1 % there.

Both the highest-wave curve EGK and FHJ, the curve upon which a_1 assumes its maximum value, can be extrapolated to the origin. If we combine the amplitude and speed results for the highest wave in deep water, we obtain the value

$$c^2/gA = 1{\cdot}348 \quad \text{for} \quad r_0 = 0, \quad (A/L) = (A/L)_{\max}. \tag{5.1}$$

This value should still be approximately correct when the depth is large but finite. From (5.1) we can obtain the linear relation

$$A/d = 0{\cdot}742c^2/gd. \tag{5.2}$$

We show a segment of this line, labelled $(A_{\max})_0$, in figure 6. It is clearly the correct asymptote for *EGK*.

Using the values of $(A/L)^*$ and a_1^* from table 2, the domains of convergence of the two expansions have been delineated. The series expansion in h converges in the region *OEGI*. It includes the highest wave for $r_0 < 0{\cdot}32$. Note that the right boundary *GHI* meets the pivotal point *I* with vertical slope. The entire domain lies within the sector $c^2/gd \leqslant 1$. The original Stokes expansion in a_1 has been found to converge in the region *OFHJI*. This region extends well into the super-critical velocity range $c^2/gd > 1$. It never includes the highest wave. These domains of convergence are not significant from a computational point of view, and result, in large measure, from the inadequacies of the Taylor series expansion. We believe that the full family of free-surface waves of finite wavelength is included within the analytic continuation of the Stokes expansion. Our ability to compute high waves in shallow water is limited only by round-off error associated with finite computer word size. The round-off error is determined by the radii of convergence and hence by the non-physical singularities.

When we are interested in the region somewhat below *FHJ*, the $a_{1\max}$ curve, either perturbation solution may be used. For $r_0 = 0{\cdot}8$ and $0{\cdot}9$, we have drawn the curves using the expansion in a_1. For these two cases the round-off error is less destructive for the a_1 expansion because its radius of convergence is larger.

We cannot, of course, compute the solitary wave with a Stokes expansion, but we shall suggest a simple extrapolation, if only to show the approximate size of the unknown region in figure 6. On the free surface of a solitary wave, infinitely far from the crest, y is zero and the velocity is c. The Bernoulli condition applied to the highest solitary wave yields the relation

$$(A/d)_{\max} = (\tfrac{1}{2})c^2/gd \quad \text{for} \quad r_0 = 1. \tag{5.3}$$

We show a segment of this straight line in the upper right corner of the figure. The speed and height of the highest solitary wave will be the co-ordinates of the intersection of (5.3) and curve *EGK*. The point denoted by the letter *S* is the highest solitary wave of Yamada (1957*b*). It is clear that an extrapolation of *EGK* will intersect (5.3) close to Yamada's point.

The complete flow field may be computed once the transformation coefficients a_i in (2.3) are known to high order. Accurate values for the a_i may be determined by summing the series $\Sigma\alpha_{ij}h^{i+2j}$ with Padé fractions for a given value of h. Then the power series in ζ is itself recast as a Padé fraction. Streamlines in the ζ plane are the circles $r =$ constant and the equipotentials are the rays $\chi =$ constant. For fixed r, a streamline may be traced parametrically as $x(\chi)$ and $y(\chi)$, $-\pi \leqslant \chi \leqslant \pi$, by separately equating real and imaginary parts of (2.3).

Figure 7 shows the results of a sample calculation for $A/L = 0{\cdot}06478$ and $r_0 = 0{\cdot}5$, corresponding to $d/L = 0{\cdot}110$. The wave height chosen is 81 % of the maximum for this depth. The first 18 coefficients a_i were summed with [7, 7]

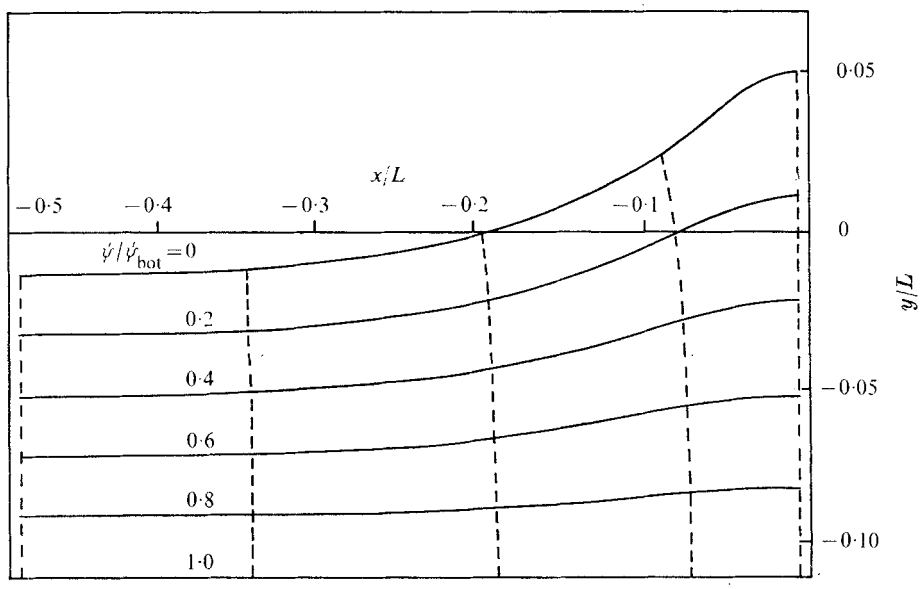

FIGURE 7. Sample flow field. $d/L = 0{\cdot}110$, $A/L = 0{\cdot}065$.

approximants. The power series in (2.3) was then recast as an [8, 8] approximant. By comparing the input wave height with the output result (i.e. examining $y(0) - y(\pi)$) an indication of the error could be obtained. The inconsistency between the two numbers was 0·06 %. If the series in (2.3) is approximated by the 18-term polynomial rather than the Padé fraction, this error is 1·3 %. The region of greatest error for the truncated series is the vicinity of the wave crest. There the lack of higher-order harmonic content is felt most acutely. The streamlines are the solid curves and equipotentials the dashed curves in figure 7. Tables of results and details of the calculation may be found in the author's Ph.D. dissertation.

6. Extended results for the deep-water wave

More detailed results have been obtained for the case of infinite depth. Qualitative aspects of these results may be expected to hold for other values of depth as well.

Table 3 shows the square of the wave speed and Bernoulli constant for various wave heights. The higher-wave results are emphasized. These numbers were computed with well-converged Padé fractions and are accurate to the number of places shown. In the immediate vicinity of $(A/L)_{\max} = 0{\cdot}1412$ only three-figure convergence could be obtained. The result for c^2 for $A/L = 0{\cdot}14$ compares well with Yamada's (1957*a*) highest-wave value 1·1931.

For the deep-water wave, equation (3.6) for the displacement of the still-water level can be shown to reduce to

$$\bar{y} = D - d = \tfrac{1}{2}(K - c^2). \tag{6.1}$$

A/L	c^2	K
0	1	1
0·04	1·01592	1·03145
0·07	1·04955	1·09533
0·10	1·10367	1·19111
0·12	1·15182	1·26790
0·13	1·17820	1·30546
0·135	1·18996	1·32017
0·14	1·1930	1·3207

TABLE 3. c^2 and K versus wave height; infinite depth

Thus table 3 can be used to compute the mass transport per wave cycle for each value of the wave height.

Figure 8 shows the variation of the first four transformation coefficients with wave height. Each a_j reaches a maximum before the maximum wave height is achieved. The location of this maximum moves to the right with increasing j. In the case of a_4, this maximum is very near $A/L = 0{\cdot}14$, the value at which numerical convergence begins to fail. As the wave profile becomes increasingly steep, the radius of curvature of the crest decreases, becoming zero for the highest wave. The a_j increase in general with wave height but, because no Fourier coefficient can cancel the contribution of any other, the steeper waves must have proportionately greater high-order harmonic content. Thus each coefficient increases until the decreasing crest radius forces it, ultimately, to recede.

Deep-water wave profiles for four values of the depth are shown in figure 9. The profiles for $A/L = 0{\cdot}030$, $0{\cdot}100$ and $0{\cdot}130$ were computed in a manner analogous to that used for the flow field of figure 7. Here the coefficients a_j were summed by [7, 7] approximants. Then the profiles were found by recasting the series in e^{ix} as a [14, 14] approximant. The inconsistency between input and output values of the wave height is 0·02 % for $A/L = 0{\cdot}130$. The highest-wave profile required a method of 'series completion' which will be described below. The profiles shown in figure 9 were taken from a group of 20 computed for various wave heights in deep water. Each profile exhibited only one inflexion point, whose distance from the crest decreased with increasing wave height. The maximum profile inclination was a monotonically increasing function of wave height. While profiles with maximum inclinations greater than 28° could not be computed accurately with [14, 14] approximants, an extrapolation to $(A/L)_{\max}$ indicates a maximum inclination very close to 30°.

Havelock (1919) included a modification of Michell's method to treat waves short of the highest. He assumed that the limiting singularity, found at the crest for the highest wave, would change in location but not in type when lower waves were calculated. If a solution for a wave short of the highest were continued analytically above the free surface a kinked streamline with the same 120° crest angle would ultimately be found. He assumed, in effect, an expansion of the form

$$q = c(1-\zeta/\zeta_0)^{\frac{1}{3}}(1+b_1\zeta+b_2\zeta^2+\ldots) \tag{6.2}$$

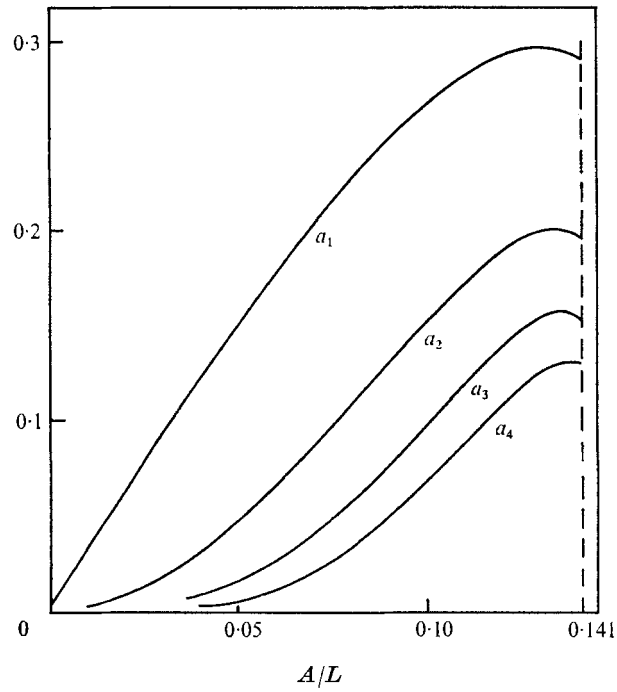

FIGURE 8. First four transformation coefficients a_i *vs.* wave height; infinite depth.

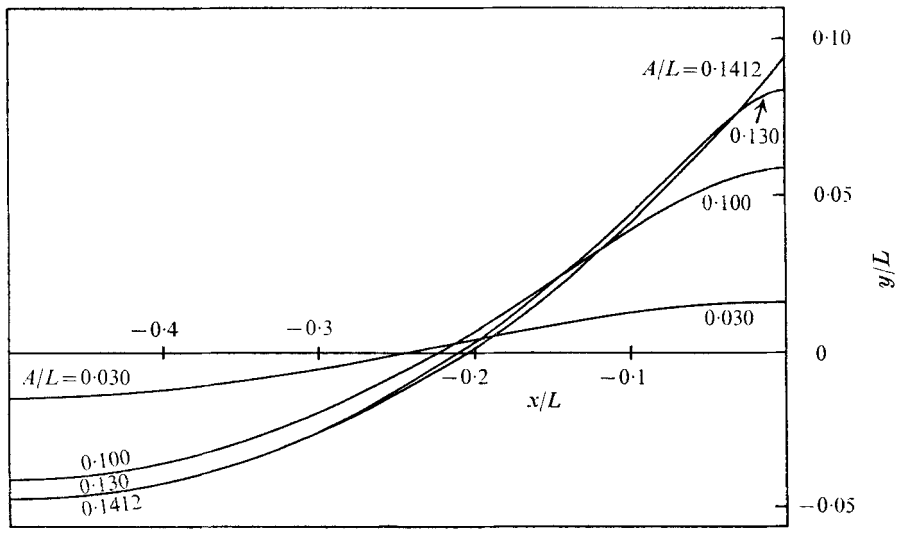

FIGURE 9. Wave profiles for the deep-water wave (oriented with respect to the still-water level).

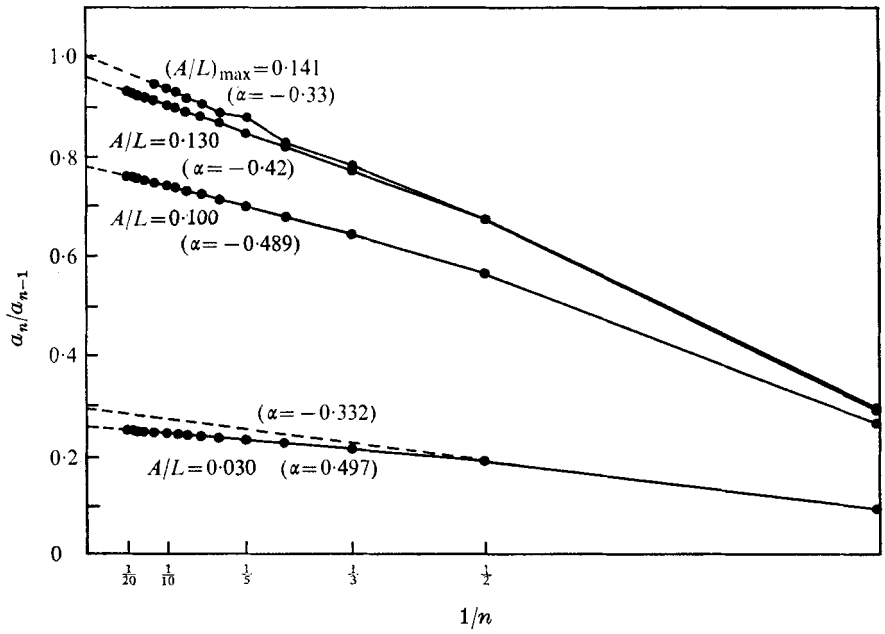

FIGURE 10. Domb–Sykes plots for the series $c/q = \sum_{n=0}^{\infty} a_n \zeta^n$; infinite depth.

for the deep-water case. The b_j, as before, would be found by satisfying the Bernoulli condition to successively higher order on the free surface $r = 1$. When $\zeta_0 = 1$, the highest wave would be found. As ζ_0 increased, lower waves would be calculated, culminating with the infinitesimal wave as ζ_0 approached infinity. Havelock also showed that, for waves of vanishingly small height ϵ, the cube-root singularity immediately satisfies the surface condition to order ϵ^2 when ζ_0 is suitably chosen.

By the use of our high-order solution and the Domb–Sykes plots, we can determine the singularity exponent and ζ_0 directly and thus assess the validity of Havelock's procedure. For the four waves whose profiles are shown in figure 9 we have drawn Domb–Sykes plots for a_n/a_{n-1} in the series

$$c/q = 1 + a_1\zeta + a_2\zeta^2 + \ldots. \tag{6.3}$$

They are shown in figure 10. For the highest-wave case, the calculation of the coefficients a_n required the use of Padé fractions formed from a solution of order h^{115}. Moreover, the actual wave height used was $A/L = 0{\cdot}1410$, slightly below the maximum. The sequence of Padé fractions gave the convergent estimates $a_1 = 0{\cdot}2917$ and $a_2 = 0{\cdot}194$. Higher-order a_n could be estimated less well and no estimates were possible for $n > 12$.

The curves in figure 10 can be extrapolated to the vertical axis to yield values of ζ_0 and the singularity exponent α. For $A/L = 0{\cdot}141$, the values are $\zeta_0 = 1{\cdot}00$ and $\alpha = -0{\cdot}33$ as expected. But for the other three cases, $A/L = 0{\cdot}130$, $0{\cdot}100$ and $0{\cdot}030$, we get $\alpha = -0{\cdot}42$, $-0{\cdot}489$ and $-0{\cdot}497$ respectively. Thus it appears that as A/L is reduced the exponent α approaches $-\frac{1}{2}$. Similar plots have been

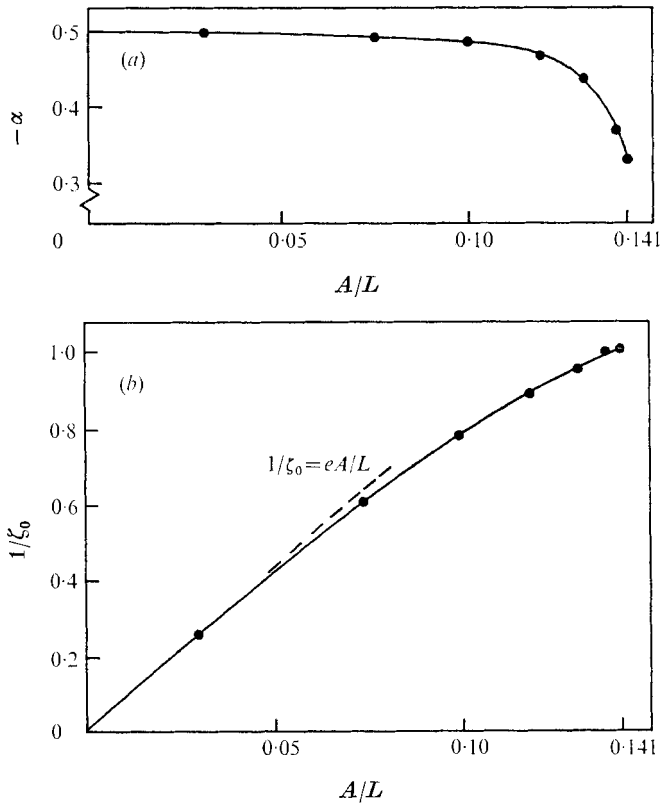

FIGURE 11. Nature and location of the limiting singularity in the ζ plane; $c/q \sim (\zeta_0 - \zeta)^\alpha$; infinite depth. (*a*) Singularity exponent. (*b*) Singularity location.

made for several other values of A/L. The results are shown in figure 11. In figure 11(*a*) we show the variation of α with wave height. It appears, from this figure, that, except for waves quite near the highest, the value $\alpha = -\frac{1}{2}$ is more nearly correct than $-\frac{1}{3}$. Figure 11(*b*) shows the location ζ_0 of this singular point. It moves from 1, for the highest wave, smoothly to infinity as the wave height decreases.

We can show that the square-root singularity must be correct for waves of small height. For the deep-water wave the result of Wilton (1914) gives

$$a_n = (n^n/n!)\, h^n + O(h^{n+2}). \tag{6.4}$$

Thus for h small and n large

$$\begin{aligned} a_n/a_{n-1} &\cong [n/(n-1)]^{n-1} h \\ &\cong eh[1 - 1/2n - 1/24n^2 + \ldots], \end{aligned} \tag{6.5}$$

where e is the base of natural logarithms. Comparing (6.5) with the equation of the straight-line asymptote on a Domb–Sykes plot

$$a_n/a_{n-1} = (1/\zeta_0)\,[1 - (1+\alpha)/n],$$

we find that, for h small and n large,

$$\alpha = -\tfrac{1}{2}, \quad \zeta_0 = 1/eh.$$

The value $\alpha = -\frac{1}{2}$ corresponds to an included angle of 90°, rather than 120°, on the broken 'streamline' in the analytic continuation of the flow, above the free surface, in the z plane.

For the lowest wave in figure 10, $A/L = 0{\cdot}030$, the coefficients a_n will differ little from the values obtained from (6.4). Notice that the slope of the straight line segment connecting the first two points, $n = 1$ and 2, yields the misleading result $\alpha = -0{\cdot}33$, explaining why Havelock was able to get second-order accuracy from the cube-root assumption. The cube-root result for low waves is fortuitous and indeed would not have been obtained had any depth other than infinity been selected.

The square-root character of the leading singularity has been found independently by Grant (1973), who also states that only square-roots can be admitted by the surface condition. The apparent continuous transition to the cube-root as shown by the results of the Domb–Sykes plots in figure 11(*a*) must then be caused by coalescense of several square-roots.

The question is open as to whether Havelock's expansion (6.2) can converge in spite of this defect. We feel that it does, if only because it has as many disposable constants as Stokes' series. Thus it should be possible to satisfy the surface condition to increasing order by their judicious selection. But, because it has the wrong singularity built in, it cannot be expected to converge much faster than Stokes' series. Since it is a great deal more difficult to evaluate Havelock's b_n than Stokes' a_n, the method is, at best, of little use.

While the method of Padé fractions yields accurate profiles for wave heights somewhat short of the maximum, it is insufficient for the description of very high waves. Padé fractions do not converge well in the immediate neighbourhood of branch-points; moreover, only the first few coefficients a_n can be determined with acceptible accuracy. A method of series completion similar to the one used by Van Dyke (1970), based on the results of Domb–Sykes plots, can be used instead. Unknown higher-order coefficients are replaced by their counterparts from the expansion of $(\zeta_0 - \zeta)^\alpha$. For a given value of the wave height, α and ζ_0 can be found from figure 11. If only the first N coefficients a_n are known, the expansion for c/q may be approximated as

$$c/q \cong 1 + \sum_{n=1}^{N} a_n \zeta^n + B \sum_{n=N+1}^{\infty} (-1)^n \binom{\alpha}{n} \zeta_0^{\alpha-n} \zeta^n, \tag{6.6}$$

where $\binom{\alpha}{n}$ are binomial coefficients in the usual notation. Since $c/q = -i\zeta dz/d\zeta$, equation (6.6) may be integrated to yield the wave profile and streamlines. The constant B is selected so that the peak-to-through wave height from (6.6) agrees with the input value.

The highest-wave profile in deep water has been drawn using this series-completion method. Here $A/L = 0{\cdot}1412$, $\zeta_0 = 1$ and $\alpha = -\frac{1}{3}$. Figure 12 compares our results for $N = 0$ and 2 with Yamada's (1957*a*) profile. For $N = 2$ we use the previously determined values $a_1 = 0{\cdot}2917$ and $a_2 = 0{\cdot}194$. Our profile with $N = 2$ is graphically indistinguishable from that of Yamada.

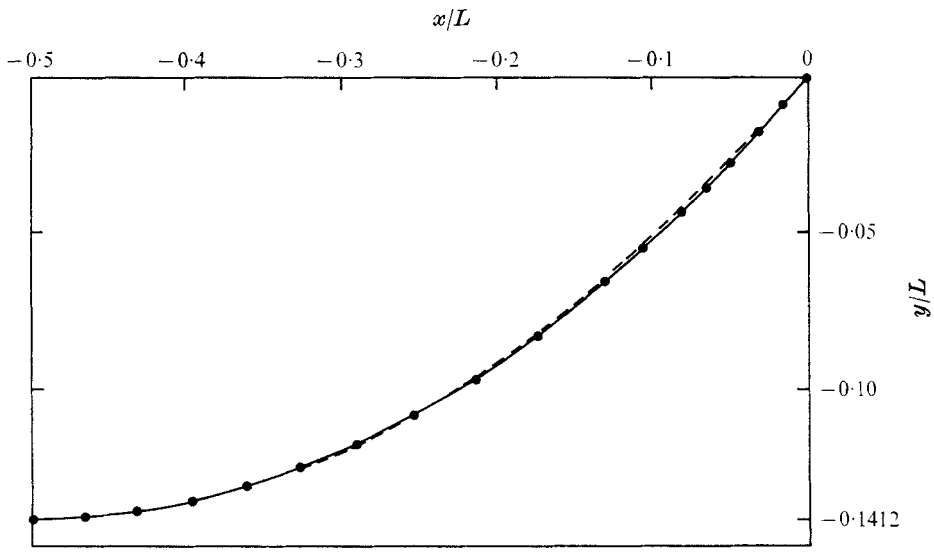

FIGURE 12. Highest-wave profile; infinite depth. ——, series-completion method, $N = 2$; – – –, series-completion method, $N = 0$; ●, Yamada (1957*a*).

7. Conclusions

The major result of the present work is that virtually all progressive free-surface waves, that is almost the entire two-parameter family, may be computed to high accuracy using the infinitesimal-wave expansion. The only exception would be large amplitude waves in very shallow water. We have no reason to believe that any 'natural barriers' exist, however, and feel that the only limitation is a practical one, based on computer word size. Admittedly, the infinitesimal-wave expansion is best suited to deep water; yet our results for shallow water are so encouraging that we believe that greater accuracy can often be achieved with the present method than with the conceptually more difficult shallow-water theories. We have obtained highest-wave results for depth/wavelength as small as 0·057 and results for waves of moderate height for $d/L = 0{\cdot}017$. All our results indicate, see figure 6 for example, an orderly two-parameter family where deep- and shallow-water waves differ mainly in scale rather than type.

We have found the radii of convergence of the infinitesimal-wave expansion where either Stokes's parameter a_1 or the wave height itself is used as the independent parameter. In our view these domains are mainly a reflexion of the inadequacy of the power-series representation. The analytic continuation provided by the use of Padé approximants renders either expansion useful over a much larger range of wave heights and water depths. The expansion in a_1 is unable to compute very high waves because a_1 is not a monotonically increasing function of wave height. By way of compensation the a_1 expansion is slightly preferable in very shallow water, where its coefficients suffer less from the effects of round-off error.

Our computation of maximum wave height versus water depth agrees well with the results of the two highest-wave-only methods. We choose to locate these

maxima as those values of the height for which the reciprocal of the crest velocity becomes singular. The method works well even when this point lies far outside the circle of convergence of the power series. We have determined, by direct calculation of the deep-water wave, that the maximum surface slope increases monotonically with the wave height.

While computing waves in shallow water, we discovered other singularities in the series expansions. Since they did not correspond to flow-field singularities, i.e. positive real values of the wave height, we made no effort to identify and remove them, relying instead on the Padé approximants to provide the necessary analytic continuation. Yet it is their presence which causes the round-off error responsible for the ultimate failure of the method to produce accurate results for high waves in very shallow water.

We have examined an alternative method proposed by Havelock for waves short of the highest. He inserts, in his expansion, the singularity corresponding to the 120° highest-wave crest angle. For waves of lesser amplitude, he places this same limiting singularity above the free surface, in the analytic continuation of the flow field. By the use of the Domb–Sykes plot and direct computation, we have shown that the 'singularity angle' decreases rapidly with wave height reaching a limiting value of 90° for the infinitesimal wave.

The author is indebted to Professor M. D. Van Dyke for his encouragement and valuable advice during the course of this research. Support was provided by a N.A.S.A. Traineeship and by the Air Force Office of Scientific Research under Contract F 44620-69-C-0036.

REFERENCES

BAKER, G. A. 1965 The theory and application of the Padé approximant method. In *Advances in Theoretical Physics* (ed. K. Breuckner), vol. 1, p. 1. Academic.

BENJAMIN, T. B. & FEIR, J. E. 1967 *J. Fluid Mech.* **27**, 417.

BOUSSINESQ, J. 1871 *C. R. Acad. Sci., Paris*, p. 755.

CHAPPELEAR, J. E. 1959 *U.S. Army Corps Engrs, Beach Erosion Bd, Tech. Memo.* no. **116**.

DE, S. C. 1955 *Proc. Camb. Phil. Soc.* **51**, 713.

DOMB, C. & SYKES, M. F. 1957 *Proc. Roy. Soc.* A **240**, 214.

GERSTNER, F. J. v. 1804 *Abh. bohm. Ges. Wiss.* **1** (3) **1**.

GRANT, M. 1973 *J. Fluid Mech.* **59**, 257.

HAVELOCK, T. H. 1919 *Proc. Roy. Soc.* A **95**, 38.

KELLER, J. B. 1948 *Comm. Appl. Math.* **1**, 323.

KORTEWEG, D. J. & DE VRIES, G. 1895 *Phil. Mag.* **39** (5), 422.

KRASOVSKII, YU. P. 1960 *Dokl. Acad. Nauk SSSR*, **130**, 1237.

MICHELL, J. H. 1893 *Phil. Mag.* **36** (5), 430.

NEKRASOV, A. I. 1921 *Izv. Ivanovo-Voznesensk. Politekhn. Inst.* **3**, 52.

SCHWARTZ, L. W. 1972 Ph.D. dissertation, Stanford University.

SHANKS, D. 1955 *J. Math. & Phys.* **34**, 1.

STOKES, G. G. 1849 *Trans. Camb. Phil. Soc.* **8**, 441.

STOKES, G. G. 1880 *Mathematical and Physical Papers*, vol. 1, p. 314. Cambridge University Press.

VAN DYKE, M. 1970 *J. Fluid Mech.* **44**, 365.

WEHAUSEN, J. V. 1965 Free surface flows. In *Research Frontiers in Fluid Dynamics* (ed. R. J. Seeger & G. Temple), p. 534. Interscience.

WHITHAM, G. B. 1967 *J. Fluid Mech.* **27**, 399.

WILTON, J. R. 1914 *Phil. Mag.* **27** (6), 385.

YAMADA, H. 1957*a* *Rep. Res. Inst. Appl. Mech., Kyushu University*, **5** (18), 37.

YAMADA, H. 1957*b* *Rep. Res. Inst. Appl. Mech., Kyushu University*, **5** (18), 53.

YAMADA, H. & SHIOTANI, T. 1968 *Bull. Disas. Prev. Res. Inst., Kyoto University*, **18** (135), 1.